Improving the Performance of Efficient Electro-Hydraulic circuit in Energy Saving Using ANN

Ayman A. Aly, Kamel A. shoush and Farhan A. Salem

Abstract— In the past few years, considerable effort has been made to improve the power efficiency of electrohydraulic systems; many energy saving strategies have been successfully developed and used. However, most of them can only be useful in specific applications. For instance, displacement control and secondary control only focus on those systems in which the efficiency concerns are more important. Although these systems have very high efficiency, they are not designed for applications in which the flow rate is varied during the duty cycle. Compared with pump controlled systems and other energy efficient systems, the valve controlled system demonstrates good dynamic performance and controllability especially for inertia dominated loads but at the expense of power efficiency. In this study, the performance of soft computing methodology, trained Artifcail Neural Network (ANN) based on the classical PID controller, is used for the control of a swash plate displacement while the compensation of the effect of the back up pressure is implemented by inverse ANN model. The feasibility of system is simulated and issue of implementation such pumps control is established. It is seen that the use of the proposed methodology results in some desirable characteristics.

Index Terms— Electro-Hydraulic circuit, Energy Saving, Artificial Neural Network, Artificial Intelligence Technique.

1 INTRODUCTION

Hydraulic systems are used to transfer energy by converting mechanical energy to fluid energy, and then back to mechanical energy. The principle reason for converting to fluid energy is the convenience of transferring energy to a new location. Hydraulic drives have many advantages over other technologies. The ratio of weight, volume and inertia to available power is significantly lower than in electromechanical drives, especially for linear motion. The dynamic performance is superior when compared to electrical or electrical-mechanical drive systems in large power drive systems [1-3]. For those systems that require an output power larger than 10 kW and a fast response speed, hydraulic drive systems are often the appropriate choice. Hydraulic systems are especially suitable for those operations characterized by abrupt loading, frequent stops and starts, reversing and speed variations that cause sharp peak, cyclic and fluctuating power demands. These advantages make them very popular in applications such as aircraft, mobile equipment, lifting machines and forest machines.

Mobile working machines play an important role in modern industry. These machines are widely used for instance in the mining, process and goods manufacturing industry, forest harvesting, harbour terminal work, telehandeler machine and tractor bachoe. Figure 1 illustrates typical examples of mobile working machines.

The heart of any electrohydraulic system is its pump. From the energy consumption point of view, pumping systems account for nearly 20% of the world's energy used by electric motors and 25% to50% of the total electrical usage in certain industrial facilities, [1]. Clearly, pumping systems consume a significant amount of the total electrical energy. The combined total of United States and Canadian energy efficiency program budgets for ratepayer funded electric and gas programs reached nearly $6.2 billion in 2009, [2].

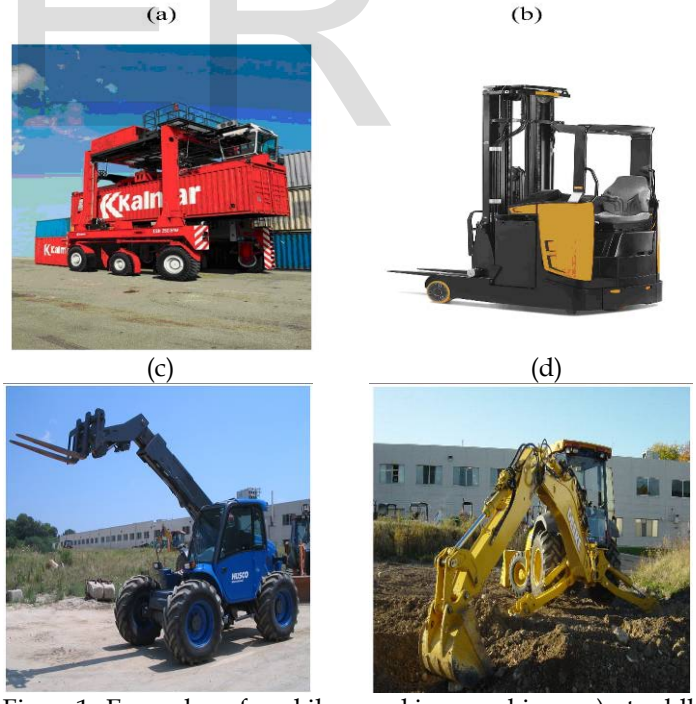

Figure1. Examples of mobiles working machines: a) straddle carrier, b) forklift truck, c) telehandeler machine and d) tractor bachoe.

Figure 2 illustrates the energy use in a typical pumping system. From the energy use, the opportunity to save energy is illustrated by the size of the percentage. The figure says that only 8% of the energy produces valuable work. The remaining

Ayman A. Aly, Kamel A. Shoush and Farhan A Salem are currently with College of Engineering, Taif university, Taif, 888, Saudi Arabia.
E-mail: draymanelnaggar@yahoo.com.
Permenant address of Ayman A. Aly is Mechanical Eng. Dept., Faculty of Engineering, Assiut university, Assiut, 71516, Egypt
Permenant address of Kamel A. Shoush Electrical Eng. Dept., Faculty of Engineering *Al_Azhar* University, Egypt.

92% is wasted energy and available for more efficient operation. The motor accounts for only 8% of the energy loss, and yet that is the main target for energy reduction in systems today through a history of both utility incentives as well as legislation.

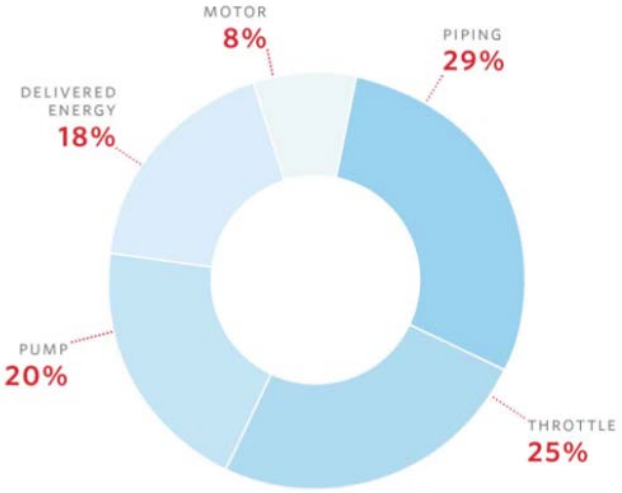

Figure 2. Energy use in a typical system, [2].

For instance, displacement control and secondary control only focus on those systems in which the efficiency concerns are more important. Although these systems have very high efficiency, they are not designed for applications in which the flow rate is varied during the duty cycle. Compared with pump controlled systems and other energy efficient systems, the valve controlled system demonstrates good dynamic performance and controllability especially for inertia dominated loads but at the expense of power efficiency. For electrohydraulic circuits which employ load-sensing systems for example, the design objective has been made to combine the advantages of high dynamic performance with better energy utilization. However, this high efficiency can only be obtained under particular operating conditions, such as single-load or multi-loads with similar load pressure requirements. No one approach is available for general system design where both good dynamic performance and high-power efficiency are important.

Industrial applications increasingly require electrohydraulic systems that offer a combination of high force output, large workspace and high accuracy. Typical applications include robotic manipulators, motion simulators, injection molding, and material testing machines, [1-10]. Electrohydraulic circuits with fast dynamic response are often characterized by low power efficiency; on the other hand, energy-efficient circuits under certain circumstances, can demonstrate slow transient responses. Continuously rising energy costs combined with the demand on high performance has necessitated that hydraulic circuits become more efficient yet still demonstrate superior dynamic response. However, the continuing success of electrohydraulic systems over competing drive technologies is contingent upon surpassing traditional performance levels, both in terms of physical measures such as motion precision and in terms of economic measures such as product cost.

Variable displacement piston pumps have found widespread application in the field of fluid power industry. The most common way to vary the flow rate of a pump is to vary its "displacement" or "piston stroke" when it is operated under a constant rotational speed. A variable displacement pump is designed such that the displacement can be varied from zero to some maximum value while the pump is operating. Changing the angle of the swashplate can change the piston stroke. Since the displacement of the pump is proportional to the piston stroke, the displacement can be changed by varying the angle of the swashplate, [6].

Several investigators [7, 8] have applied research about the dynamic properties of a variable displacement piston pump. Most of these investigations are based on a linearized model of the pump dynamics. In industrial application, the dynamic characteristics of the variable delivery pump are always complex and highly nonlinear, [6]. Moreover, there are too many uncertainties in it; as the viscosity of the oil, the bulk modulus, leakage coefficient, equivalent torque coefficient, volumetric displacement and others. So, the design of such pumps control flow at different pump pressure levels needs various controllers that cause the pump output to match different load characteristics more efficiently and effectively. The design of these controllers, however, is often based on compromise and thus their performances are very operating condition dependent.

Soft computational methods have become very popular recently involving mapping of input-output vectors for cases where no theoretical model works satisfactorily. An artificial ANN [11-17] is an information-processing paradigm inspired by the manner in which the heavily interconnected, parallel structure of the human brain processes information. They are collections of mathematical processing units that emulate some of the observed properties of biological nervous systems and draw on the analogies of adaptive biological learning. ANNs are trainable systems whose learning abilities, tolerance to uncertainty and noise, and generalization capabilities are derived from their distributed network structure and knowledge representation. Learning of a ANN typically implies adjustments of connection weights and biases so that the square error (between ANN output and desired output) is minimized.

In this search, it is objected to carry out the following:

1. Design a classical control policy as a comparative base
2. Design the proposed intelligent control strategy.
3. Study the performance of efficient electro-hydraulic circuit Control in energy saving.

2 DC Motor Controlled Pump Model

One approach to model a dynamic system is to use linear or small signal analysis. The linear analysis method is based on the assumption that a linear transfer function can be used to describe the behavior of the plant over the complete operating range. On the other hand, the small signal analysis method assumes that the plant behavior is nonlinear but the model can

be linearized over a small range near an operating point. Both methods are very powerful analytical tools but have limitations, especially for a highly nonlinear dynamic system such as the DC motor controlled pump. In this study, the pump is modeled using nonlinear large signal techniques which are represented by a series of differential equations. Although it is difficult to analyze the dynamic performance of a nonlinear model using conventional control theories (transfer function approaches), it is feasible to do this using a simulation program.

The flow rate is determined by the angle of the swashplate which, is controlled using a permanent magnet servo DC motor, [2]. From the viewpoint of the pump control, the DC motor can be considered as a part of the pump. Hence, the model of the DC motor is also a part of the pump model.

The mathematic model of a DC motor can be derived using a schematic diagram of the motor circuit shown in Fig.3. The DC motor is assumed to consist of inertia, Jd, with damping, Bd. The torque developed by the current in motor windings not only overcomes the friction in the DC motor and load torque, Tdl, on the motor shaft but also accelerates the rotor, [10].

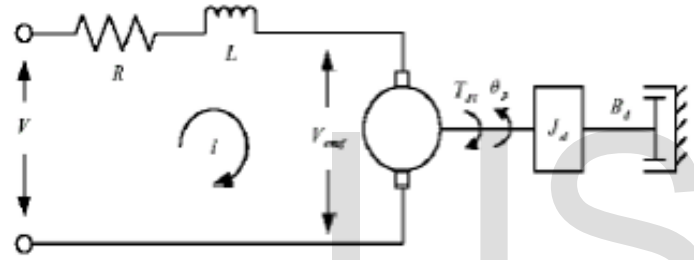

Figure 3. Schematic diagram of a DC motor

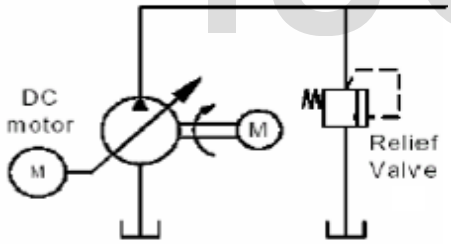

Figure 4. Pump-controlled system with relief valve

The electrical circuit of the motor can be simply described by:

$$V = V_{emf} + Ri + L\frac{di}{dt} \quad (1)$$

$$V_{emf} = K_b \dot{\theta}_p \quad (2)$$

The torque developed at the shaft of the motor is proportional to the armature current and given by:

$$K_t i = J_d \ddot{\theta}_p + B_d \dot{\theta}_p + \mathrm{sgn}(\dot{\theta}_p)(T_{ds} + T_{dc}) + T_{dl} \quad (3)$$

The friction torque consists of three terms: static friction, coulomb friction, and viscous damping. Normally, the static friction and coulomb friction of the DC motor are negligible compared to that of the pump swashplate. This is evident by the effortless torque that is required to manually turn only the shaft of the DC motor.

Neglecting the static and coulomb friction and taking Laplace transforms of equations 1 to 3 yields the model of the DC motor as described by the following transfer function.

$$\theta_p(s) = \frac{K_t V(s) - (Ls + R)T_{dl}(s)}{s((Ls + R)(J_{dm}s + B_{dm}) + K_t K_b)} \quad (4)$$

The numerator of equation 4 includes two terms. One term is the input signal and the other one is the load, which can be considered as a "disturbance" input signal.

In 1987, Kavanagh [4] developed a comprehensive model for a variable displacement axial piston pump which is used as the basis for modeling the pump in this study. The pump model consisted of the torque model and fluid flow model. The motion of the swashplate is described by the torque model; and the flow rate of the pump is described by the flow model.

Some general assumptions are made regarding the pump model. They are:

- Constant prime drive speed on the pump,
- Zero suction and drain pressure,
- Constant chamber volume
- Constant fluid density and temperature.

In Kavanagh's study, the swashplate is controlled by a control piston and balanced by a return spring. However, in this study, the swashplate is actuated by a DC motor. Under these conditions, Kavanagh's model can be simplified to yield

$$J_p \ddot{\theta}_p = T_d - S_1 - S_2\theta_p - sgn(\dot{\theta}_p)T_{fc} - B_p\dot{\theta}_p - K_{p1}P_p - K_{p2}P_p\theta_p \quad (5)$$

The displacement of the pump is defined as follows:

$$D_p = NA_pR_P \tan\theta_p / \pi \quad (6)$$

Assuming that the rotational speed of the prime mover is ωp, the ideal flow rate of the pump is as follows:

$$Q_{pidea} = \omega_p D_p = \omega_p NA_p R_p \tan\theta_p / \pi \quad (7)$$

The actual flow rate of the pump is less than the ideal flow rate due to the fluid leakage and fluid compression. There are two types of leakage flows in the pump, one is the internal leakage flow between the suction port and the discharge port of the pump and the other is the external leakage from the high-pressure chamber to the case drain through the pump casing. From the continuity equation, the flow equation of the pump can be written as

$$Q_{pidea} - Q_{ip} - Q_{ep} - Q_p = \frac{V_p}{\beta_e}\frac{dP_p}{dt} \quad (8)$$

Since the suction pressure is assumed to be zero, the leakage flow of the pump (including the internal leakage and the external leakage flow) can be approximated by

$$Q_{lp} = Q_{ip} + Q_{ep} = C_{tp}P_p \quad (9)$$

Substituting equations.7 and 9 into equation.8, yields

$$\omega_p NA_p R_p \tan\theta_p / \pi - C_{tp}P_p - Q_p = \frac{V_p}{\beta_e}\frac{dP_p}{dt} \quad (10)$$

As shown in Fig.4, there is a two-stage relief valve (RV),

worked as a constant "resistive" load. It is used to adjust the backpressure on the system.

3 Closed Loop Control System

The feedback signal is the angular position of the pump swashplate, which is also the controlled variable. The closed loop system is including a controller, a power amplifier, a DC motor and a variable displacement pump. The purpose for controlling the swashplate angle is to control the flow rate of the pump. Before designing the controller, it is important to determine the dynamic performance of the DC motor and pump swashplate assembly. As a result, a model of the DC motor and pump is attempted. Based on this model, a motor controller is designed based on Ziegler-Nichols turning PID rules, [11]. A typical PID controller has the following transfer function form,

$$G_c(s) = K_p + \frac{K_I}{s} + K_d s \tag{11}$$

As the system gains changed with pressure changes, the critical gain and oscillation frequency are not the same under different loading. It is interesting to note that at the same pressure level, the pump operation tended to be stabilized by decreasing the gain and destabilized by increasing the gain. On the other hand, at the same gain, the pump tends to be stable with increasing the pressure and unstable with decreasing the pressure. Thus, the pump demonstrates a highly nonlinear characteristic which is strongly dependent on the operating pressure and controller gains, [12].

So at every operating point a new PID gains setting is needed. However, the linear PID is difficult to apply to this highly nonlinear plant. Even with a perfect feedforward controller, a feedback controller is also required to correct for noise and unmeasured disturbances.

The requirement for the controller design at this stage is to design a DC motor controller which could drive the DC motor and pump swashplate at any pressure levels with a fast dynamic response but without exhibiting any limit cycle oscillations.

Many methods can be used to design the controller for a dynamic system; however, most of them are limited to linear systems. As a proposed solution, a ANN controller is designed using the linear PID as a teacher to it to control the system at any pressure level.

However, ANN is often called a black box, since, unlike fuzzy logic, it is difficult to interpret the knowledge stored by an ANN. Knowledge in an ANN is represented in the values of the weights and biases, which forms part of large and distributed network.

3.1 Back-Propagation Algorithm

Back-propagation learning is one of the most popular types ANN learning methods. It has two operational phases. In first phase, forwarding phase, we send input data from input layer to the output layer. In the second phase, back-propagation phase, we calculate the error (between target and output) and propagate the error backwardly to the input layer in order to change the weights of hidden layers by using the gradient descent method.

The neural network is trained, using supervised learning, to develop an inverse model of the plant is shown in Fig.5, the network input is the process output and the network output is the corresponding process input. Inverse model are typically developed with steady state data and used for solve the problem of finding the swashplate angle which will produce the required flow rate whatever the pressure level.

Several studies have found that a three-layered neural network with one hidden layer can approximate any nonlinear function to any desired accuracy [13]. The network consists of input layer, hidden layer and output layer. To explain the Back-propagation rule in detail a 3 layer network shown in Fig.6 will be used. The training phase is divided as follows:

1. forward-propagation phase: X=[Qp; PP] is propagating from the input layer to the output layer Y=[θp].

$$Z_q = f\left(\sum_{j=1}^{m} v_{qi} X_j\right) \tag{12}$$

$$Y_i = f\left(\sum_{q=1}^{l} w_{iq} Z_q\right) \tag{13}$$

2. back-propagation phase: (14) shows the error between the output, y, and the target, d.

$$E = \frac{1}{2}\sum_{i=1}^{n}(d_i - y_i)^2 \tag{14}$$

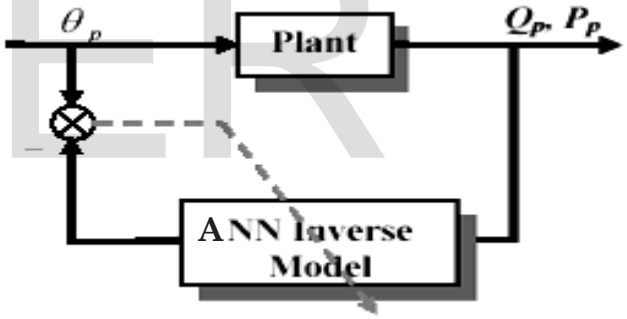

Figure 5. ANN plant inverse model

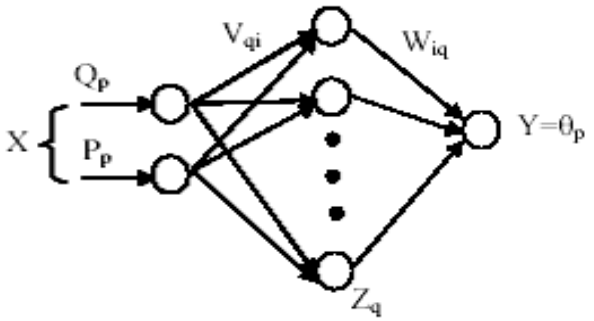

Figure 6. ANN for back-Propagation

By using the gradient-descent method, the weights in hidden-to-output connections are updated as follows:

$$\Delta w_{iq} = -\eta \frac{\partial E}{\partial W_{iq}} = -\eta\left[\frac{\partial E}{\partial Y_i}\right]\left[\frac{\partial Y_i}{\partial net_i}\right]\left[\frac{\partial net_i}{\partial W_{iq}}\right]$$
$$= -\eta[d_i - y_i]\left[f'(net_i)\right][Z_q] = \eta\delta_{oi} Z_q \tag{15}$$

Following equations are the weight update on the input-to-hidden correction. Also chain rule and gradient-descent method are employed.

$$\Delta v_{qi} = -\eta \frac{\partial E}{\partial V_{qi}} = -\eta \left[\frac{\partial E}{\partial net_q}\right]\left[\frac{\partial net_q}{\partial V_q j}\right] = \eta \delta_{hq} x_i \quad (16)$$

$$\delta_{oi} = -\left[d_i - y_i\right]\left[f'\left(net_i\right)\right] \quad (17)$$

$$\delta_{hq} = \left[\frac{\partial E}{\partial Z_q}\right]\left[\frac{\partial Z_q}{\partial net_q}\right] \quad (18)$$

In Back-propagation learning rule, the two phases are iterated until the performance error decreased to certain small range.

The proposed network consists of the three layers; the output layer consists of one neuron with linear activation function as shown in equation 19 and Fig.7.a. Numbers of neurons in the hidden layer are chosen by trial and error. We begin by five neurons but the network performance is not satisfactory. So, we increased the number to 20 neurons and the performance is improved. Increasing the number may enhance the performance, but we must bear in mind that the smaller numbers is the better in terms of both memory and time requirement to implement the ANN. The activation functions in hidden layer neurons are tan sigmoid functions which are defined in equation 20 and shown in Fig.7.b.

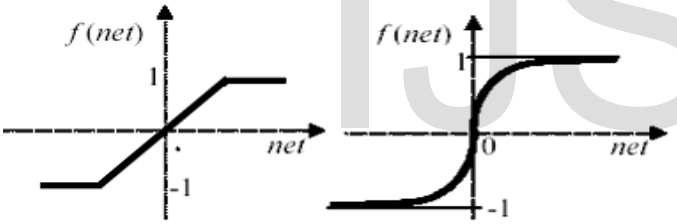

(a) Piecwise linear (b) Sigmoid

Figure 7. Activation function

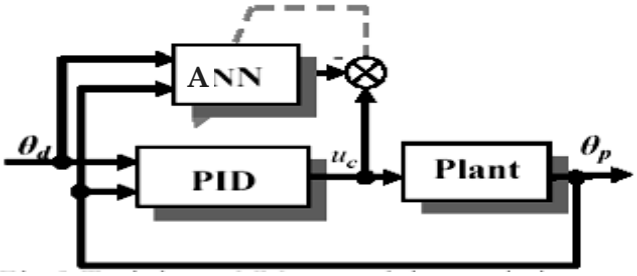

Figure 8. Training a ANN to model an existing PID controller

piecewise linear activation function

$$f\left(net\right) = \begin{cases} -1 & net < -1 \\ net & \left|net\right| \le 1 \\ +1 & net > 1 \end{cases} \quad (19)$$

Tan Sigmoid activation function

$$f\left(net\right) = \frac{1 - e^{-2net}}{1 + e^{-2net}} \quad (20)$$

Neural network can be trained to model existing controllers, a straightforward application of supervised learning. The neural network receives the same inputs as the existing controller, and the error between the neural network output and the existing controller output is back-propagated to train the neural network as shown in Fig.8.

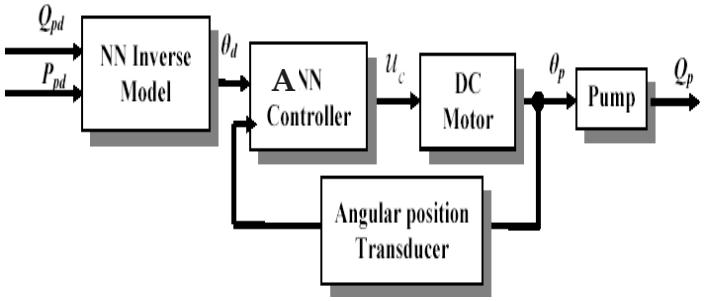

Figure 9. The ANN pump control system with the ANN inverse model

A neural network is trained off line using the previous back-propagation learning rule to mimic an existing PID controller and then is further refined in conjunction with a process model. This work is one of the major commercial successes of neurocontrol.

Figure 9 illustrates how the proposed controller is trained and implemented.

4 Results and Dissection

The proposed ANN is used to identify the inverse of system (D-C motor, amplifier, transducers, pump and load) dynamics, then we used this inverse model to generate the input voltage of reference swashplate angle to follow a pre-selected set point in flow and pressure.

The capability of ANN is trained by applying different set points of pump flow rates and pressures. Fig.10 presents the space relation of the swashplate, pump flow rate and pump pressure. As the swashplate angle is increased the flow rate is increased at the same pressure level. If the back pressure level increases it will has opposite effect in flow rate at the same swashplate set point. The resulted figure will be the base for training the inverse ANN model. It is clear from noticing the three dimensional plot that the relation is nonlinear. Fig.11 shows the target swashplate angle and the trained ANN output angle at different flow rates and pressure levels. The error signal is illustrated in Fig.12. It can be seen from the figure that the trained signal follows the desired signal very closely and the error nearly approach zero (4x10-8 m3/sec.) after 40 samples.

By using Ziegler-Nichols method the PID gains Kp, KI, and Kd will be [2100 1.9091x105 5.775], and it will produce an overshoot response of the swashplate and consequently of the pump flow rate as displayed in Fig.13 and 14. As overshoot of the pump flow rate increases, the overshoot of the hydraulic motor output and the dynamic load also will increase. So the PID control need to improve its gains setting to give minimum overshoots as possible. The trail and error technique is considered to adjust manually the PID gains to get the accepted

response of the pump flow rate.

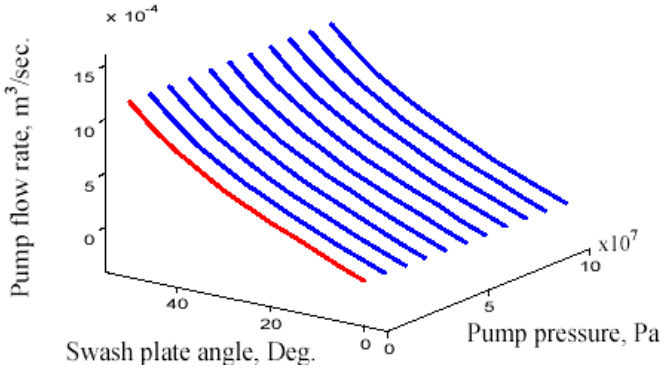

Figure 10. The training trajectory reference for the inverse ANN model

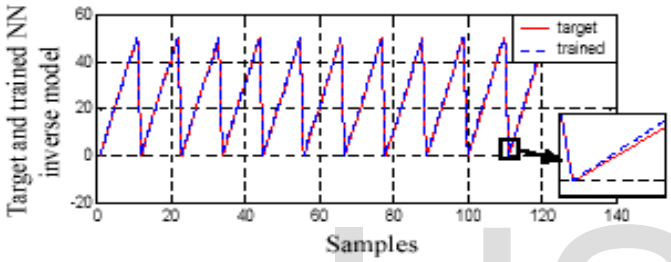

Figure 11. Orginal and trained response of the system inverse model

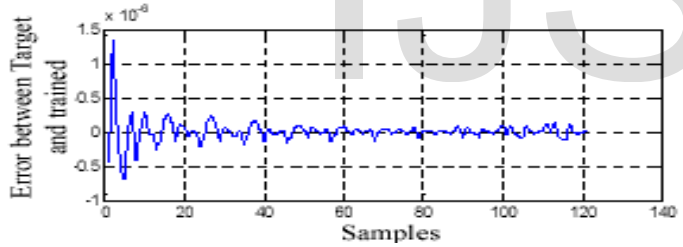

Figure 12. The error in between of the original and trained responses

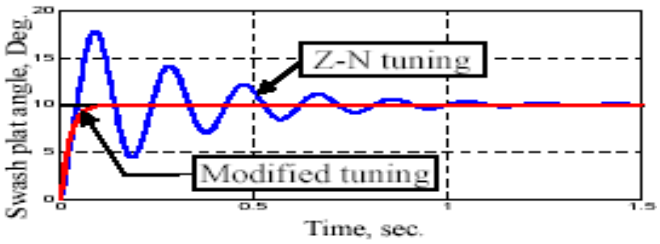

Figure 13. The sawsplate angle with reference 10 Deg. Based on PID control

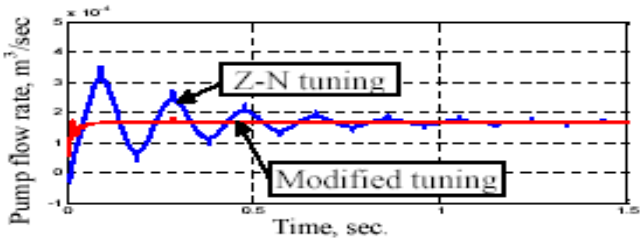

Figure 14. The pump flow rate based on PID control

The ANN controller voltage will use the modified PID controller as a teacher to it as introduced in Fig.15. The trained signal follows the target signal very closely. For testing the trained ANN controller, a reference swashplate desired trajectory is applied in Fig.16. It is illustrated that the error in between of them is 0.07 Deg at steady state. with rise time of 0.1 sec. and no overshoot achieved.

The corresponding response of the modified PID gains Kp, KI, and Kd of [900 56 0.25], is shown in Fig.17 for the pump flow rate and pressure set point of [1.5x10-4 m3/sec., 15MPa], it is noticed that the flow rate get steady state error as pressure is increased to 25MPa or 35MPa. This is reasonable result for the fact of that the controller has not a pressure compensator for these disturbance to the nominal plant. The controller signal at the lower part of Fig.17 does not respond to the changes of the pressure levels. In Fig. 18, the system response based on the proposal trained ANN controller has a robustness behavior because of at every pressure level the inverse model repeat the calculation of the adequate swashplate angle to keep the flow rate constant regardless to the pressure level.

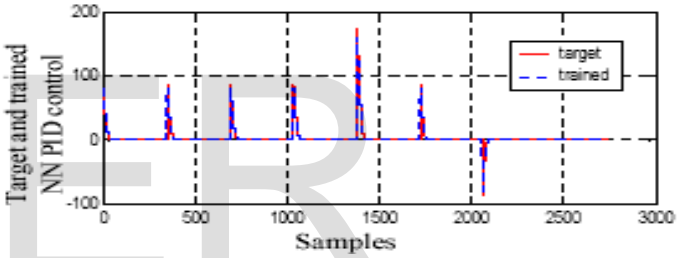

Figure 15. Original and trained signals of the PID control and the error in between

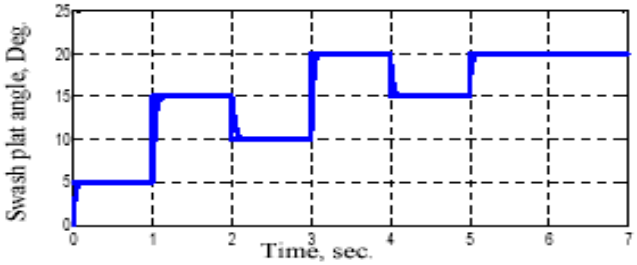

Figure 16. The swashplate angle response based on ANN control

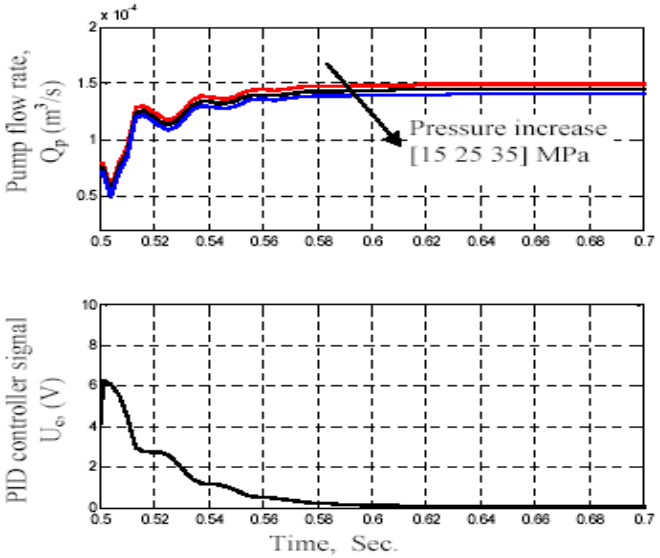

Figur 17. The system flow rates bsed on modified PID control and the controller signal with different pressure levels

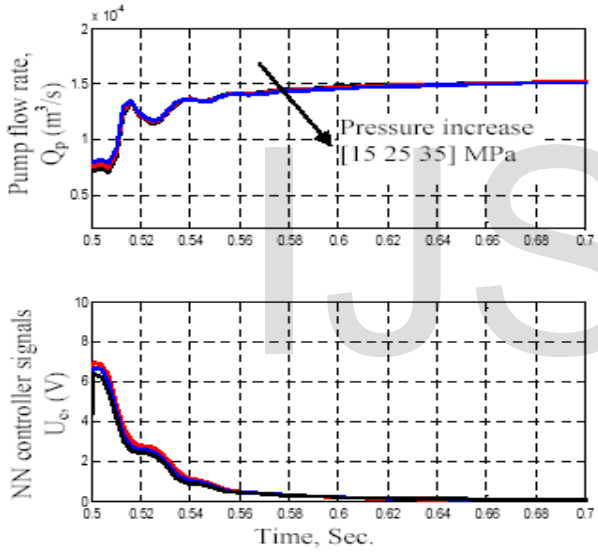

Figur 18. The system flow rates bsed on modified ANN control and the controller signal with different pressure levels

5 Conclusion

To improve the dynamic response of the pump, a DC motor is implemented to control the pump swashplate (and hence flow rate) directly. The pump and DC motor are mathematically modeled and their parameters are simulated via MATLAB 6.3 and SIMULINK 5.0 software. By means of the DC motor's quick dynamic response, the DC motor controlled pump demonstrated a fast dynamic response independent on the pump pressure.

For precise control, an off-line learning algorithm is introduced. The strategy of design is also given. It is important to note that the ANN have the distinct advantage of not relying on the system parameters and it deal with system as a black box. The simulation results indicate the accuracy of tracking. Also the effectively of the proposed controller with the inverse ANN model is cleared. It gave a robustness response, as the pressure changes, the pump does not affect to a great extent the output flow rate accuracy.

Acknowledgment

This search is supported by Taif University under a contract NO. 1-435-3047. The University is highly acknowledged for the financial support.

References

[1] Li,C.C., X.D. Lin, Zhou, X. Bao and J. Huang. Fuzzy control of electro-hydraulic servo systems based on automatic code generation. Proceeding of the 6th International Conference on Intelligent Systems Design and Applications, Oct.16-18, IEEE Computer Society, Washington DC, USA, 2006, pp. 244-247.

[2] Brent ross, " Pumping systems: low hanging fruit in energy saving, Armostrong Ltd., 2011.

[3] KwanchaiSinthipsomboon. Industrial Hydraulic, Se-education public company limited, 1987, pp. 25-87.

[4] Darrel Janesak and Dave Roepp. Hybrids make a move to the plant floor, Hydraulics & pneumatics, August 2006, pp. 32-49.

[5] Xu, M., Jin, B., Shen, H.K., Li, W. (2010). Analysis and design of energy regulation device in energy regulation based variable speed electro-hydraulic control system. Chinese Journal of Mechanical Engineering, vol. 46, no. 4, p. 136-142, DOI:10.3901/JME.2010.04.136.

[6] Shen, H.K., Jin, B., Chen, Y. (2006). Research on variable-speed electrohydraulic control system based on energy regulating strategy. ASME International Mechanical Engineering Congress and Exposition, Chicago.

[7] Merritt, H., 1967, "Hydraulic Control Systems", John Wiley & Sons, Inc., New York, pp.152-157.

[8] "HT-High Torque, Direct Drive Series", Emoteq Inc., Tulsa, Oklahoma

[9] Tonglin Shang, 2004, "Improving Performance of an Energy Efficient Hydraulic Circuit", MSc. University of Saskatchewan, Saskatoon, Saskatchewan, Canada.

[10] Kavanagh, G. P., 1987, "The Dynamic Modelling of an Axial Piston Hydraulic Pump", MSc Thesis, Department of Mechanical Engineering, University of Saskatchewan, Canada.

[11] G.S. Virk and A. Al-Dmour, Jan.1994 "System Simulation Using Neural Networks", Departmental Research Report No. 537, University of Bradford.

[12] Ayman A. Aly and Aly S. Abo El-Lail ,"Intelligent PI Fuzzy Control of an Electro-Hydraulic Manipulator", International Journal of Control, Automation And Systems (IJCAS) 3 (2), PP.19-24, 2014.

[13] Tharwat O. S. Hanafy, Al-Osaimy, Mosleh M. Al-Harthi and Ayman A Aly , "Identification of Uncertain Nonlinear MIMO Spacecraft Systems Using Coactive Neuro Fuzzy Inference System (CANFIS)", International Journal of Control, Automation And Systems (IJCAS) 3 (2), PP.25-37, 2014.

[14] Tharwat O. S. Hanafy, Al-Osaimy A. S. and Ayman A. Aly ,"Facilitation Rule Base for Solidification of Nonlinear Real Plant System", International Journal of Control, Automation And Systems (IJCAS) 3 (1),PP.1-9, 2014.

[15] Tharwat O. S. Hanafy, Ayman A. Aly and Kamel A. Shoush, "Dynamic Evolving Neuro Fuzzy Systems of Qualitative Process", International Journal of Control, Automation And Systems (IJCAS) 3 (1),PP.17-26, 2014.

[16] Tharwat O. S. Hanafy, H. Zaini, Kamel A. Shoush and Ayman A. Aly ,"Recent Trends in Soft Computing Techniques for Solving Real Time Engineering Problems", International Journal of Control, Automation And Systems (IJCAS) 3 (1),, PP.27-33, 2014.

[17] R.J. Schalkoff, 1997, "Artificial Neural Networks", McGraw-Hill, Inc.

Nomenclature

A_p	Area of the piston, (8305×10^{-6} m^2)
B_d	Viscous damping coefficient, (1.43×10^{-3} Nm.rad^{-1}s)
B_p	Damping coefficient of the swashplate yoke assembly, (0.28 Nm.rad^{-1}s)
C_{tp}	Total leakage flow coefficient, (4.3×10^{-13} m^{3}s^{-1}.Pa^{-1})
D_p	Displacement of the pump, (1.95×10^{-6} m^3.rad^{-1})
i	Armature current, (A)
J_d	Moment of inertia of the motor rotator, (1.4×10^{-3} Nm.rad^{-1}s^2)
J_p	Average moment of inertia of swashplate yoke assembly, (1.06×10^{-3} Nm.rad^{-1}s^2)
K_b	Back EMF constant of the DC motor, (2.27 V.rad^{-1}s)
K_d	Derivative gain
K_i	Integral gain
K_p	Proportional gain
K_{p1}	Pressure torque constant, (7.46×10^{-7} Nm.Pa^{-1})
K_{p2}	Pressure torque constant, (8.3×10^{-7} Nm.Pa^{-1}.rad^{-1})
K_t	Motor torque sensitivity, (2.27 NmA^{-1})
L	Terminal inductance of the DC motor windings, (0.0332 H)
N	Number of pistons, (9 pistons)
P_p	Pump pressure, (Pa)
Q_{ep}	External leakage flow of the pump, (m^{3}s^{-1})
Q_{ip}	Internal leakage flow of the pump, (m^{3}s^{-1})
Q_p	Output flow of the pump, (m^{3}s^{-1})
R	Terminal resistance of the DC motor windings, (4.83 Ω)
R_p	Radius of the piston pitch, (0.0224 m)
S_1	Simplified pump model constant, (0.096 Nm)
S_2	Simplified pump model constant, (2.36 Nm.rad^{-1}),
T_d	Torque applied to the yoke by the DC motor, (Nm)
T_{dc}	Coulomb friction torque, (Nm)
T_{dl}	Load torque acting on the DC motor shaft, (Nm)
T_{ds}	Static friction torque, (Nm)
T_e	Motor electrical time constant, (6.87×10^{-3} sec)
T_{fc}	Torque produced by the coulomb friction force, (0.36 Nm)
T_m	Motor mechanical time constant, (1.3×10^{-3} sec)
V	Input voltage, (V)
V_{emf}	back EMF voltage, (V)
V_p	Volume of the pump forward chamber, (3×10^{-5} m^3)
β_e	Bulk modulus of the fluid, (1.45×10^9 Pa)
θ_p	Angular position of the DC motor shaft and pump swashplate, (rad)
ω_p	Pump rotational speed, (183.3 rad s^{-1})
γ	Damping factor.